

## Electronic Supplementary Information

### Cancer Diagnostics via Ultrasensitive Multiplexed Detection of Parathyroid Hormone-related Peptides (PTHrP) with a Microfluidic Immunoarray

Brunah A. Otieno<sup>a,♦</sup>, Colleen E. Krause<sup>a,b,♦</sup>, Abby L. Jones<sup>a</sup>, Richard B. Kremer<sup>c</sup>, James F. Rusling<sup>a,d,e,f,\*</sup>

<sup>a</sup>*Department of Chemistry, University of Connecticut, Storrs, CT 06269*

<sup>b</sup>*Department of Chemistry, University of Hartford, West Hartford, CT 06117*

<sup>c</sup>*Department of Medicine, McGill University, Montreal, Quebec H3A 1A1, Canada*

<sup>d</sup>*Institute of Materials Science, University of Connecticut, Storrs, CT 06269*

<sup>e</sup>*Department of Surgery and Neag Cancer Center, University of Connecticut Health Center, Farmington, CT 06232*

<sup>f</sup>*School of Chemistry, National University of Ireland at Galway, Ireland.*

♦B. A. Otieno and C.E. Krause contributed equally to this article.

### Table of Contents

#### Experimental Details

#### Supplementary Figures

**Figure S1** Components of the microfluidic device

**Figure S2** Optimization of monoclonal antibody (Ab<sub>2</sub>) and polyclonal antibody (Ab<sub>1</sub>)

**Figure S3** Minimal carry-over effect between runs.

**Figure S4** Amperometric response for individual peptide fragments

**Figure S5** Multiplexing strategy for peptide fragments

**Figure S6** Cyclic Voltammogram of 8-electrode arrays in H<sub>2</sub>SO<sub>4</sub>

## **Supplementary Tables**

**Table S1** Stability of the serum samples after 6 months interval

**Table S2** Characterization of magnetic Bead Conjugate

**Table S3** Evaluation of Assay Performance

**Table S4** Detection Limit and Sensitivity

**Table S5** Serum Samples Data

**Table S6** Correlation Plot Table

## **References**

## **Experimental Details**

### **Chemicals and Materials**

Horseradish peroxidase (HRP), sterile filtered bovine calf serum, Tween-20, bovine serum albumin (BSA), gold (III) chloride trihydrate ( $\text{HAuCl}_4 \cdot 3\text{H}_2\text{O}$ , 99.9%), sodium borohydride (99%), tetraoctylammonium bromide, 3-mercaptopropionic acid (MPA), 1-dodecane thiol, poly(amic acid), 1-(3-(Dimethylamino)propyl)-3-ethylcarbodiimide hydrochloride (EDC), N-hydroxysulfosuccinimide (NHSS), hydroquinone (HQ,  $\geq 99\%$ ) and horseradish peroxidase were from Sigma-Aldrich. Hydrogen peroxide ( $\text{H}_2\text{O}_2$ , 30%) was from Fisher. Kapton FPC film (127  $\mu\text{m}$  thick) was purchased from American Durafilm. The poly(dimethoxy)silane (PDMS) kit was purchased from Dow Corning. MyOne tosylactivated beads (1  $\mu\text{m}$  diameter, Dynabeads) and were from Invitrogen. Immunoreagents (monoclonal antibodies, polyclonal antibodies, BSA) were dissolved in pH 7.4 phosphate saline buffer (PBS, 5.9 mM  $\text{Na}_2\text{HPO}_4$ , 3.9 mM  $\text{NaH}_2\text{PO}_4$ , 2.7 mM KCL, 120 mM NaCl). 400 mM EDC and 100 mM NHSS were dissolved in water immediately before use. All solutions were prepared with 18  $\text{M}\Omega \cdot \text{cm}$  water purified through use of a Hydro water purification system (Durham, NC, USA).

### **PTHrP peptides and Antibodies**

Intact PTHrP 1-173 was produced from cDNA encoding the PTHrP 1-173 isoform. Human PTHrP fragments 1-33, 151-169, 140-173 were purchased from Sheldon Biotechnology Center (McGill University). Human recombinant PTHrP 1-86 Human recombinant PTHrP 1-86 was from Bachem (Torrance, CA, cat # H-9815). Monoclonal antibodies M45 (IgM) and PA158 (IgG) were raised against PTHrP1-33; monoclonal antibody PA104 (IgG) was raised against PTHrP 140-173; monoclonal antibody PA6 (IgG) was raised against PTHrP 151-169, PA104, PA158. All monoclonal antibodies were purified by affinity chromatography (Medilabs, Quebec) and found highly specific with no cross reactivity with PTH and other unrelated peptides.<sup>1</sup> The bioactivity of these monoclonal antibodies was tested previously both in vitro and in vivo. Polyclonal antibodies against human PTHrP 1-173 (IgY lots 3103 and 3104 were raised in chicken and purified commercially (Genway Biotech, San Diego, CA).

Stock concentration of peptide standards (200 -500 ng for 1-33, 151-169, 140-173 and 1-173 from Sheldon Biotechnology Center, McGill University and PTHrP 1-86 was from Bachem (Torrance, CA, cat # H-9815). were first diluted in water or PBS buffer pH 7.4 to 50 pmol/L (1

ng/mL) and stored at -80 °C (according to the manufacturer's specifications). The antibodies were reconstituted in PBS buffer pH 7.4 down to the working concentration and stored at -80 °C. The peptides and antibodies were stable for 12 months. On assay days, one vial of 50 pmol/L peptide standard was then diluted to 1 pmol/L followed by serial dilution in 5x diluted calf serum in PBS buffer pH 7.4. The diluted standards were used the same day they were prepared and any left-over standards were discarded. In all the calibration curves 5x diluted calf serum was employed as assay diluent for serial dilutions. Current density was used for quantitation of the standards. The peak height (I, nA) was divided by the surface area of the electrode to yield the current density that was plotted against the concentration of the peptide fragments. Log fitting was used to plot the data.

### **Immunoradiometric assay (IRMA) for PTHrP**

We used a commercial PTHrP assay for correlation purposes (PTHrP RUO, Active® IRMA catalog # DSL8100 Beckman Coulter Canada Inc, Montreal, Canada). This IRMA has been previously described to measure PTHrP in various cancer stages and to establish normal control values. It uses an N-terminal monoclonal antibody raised against PTHrP1-40 and a mid-region monoclonal antibody raised against PTHrP 57-80. It has a sensitivity of 0.3 pmol/L (3 pg/mL) and linearity up to 212 pmol/L (2100 pg/mL). Internal controls were made using pooled samples and conditioned media from PTHrP producing cells lines. The inter-assay variability was 4.4% and the intra-assay variability was 4.7%, according to the manufacturer's specifications. Normal values obtained from 40 healthy volunteers range from 0-15 pg/mL (0-1.5 pmol/L).

### **Human Serum Samples**

Human serum samples from 22 healthy subjects and 37 cancer patients with solid tumors were obtained from McGill University Health Center Biorepository. Blood was drawn in regular tubes, tubes put on ice immediately and separated within 60 min, aliquoted and stored at -80 °C prior to assay. No degradation of the serum samples was observed by assaying the samples after 6 months interval. All samples used in this study were acquired under an institutional review board-approved protocol, and informed consent was obtained from all study participants.

**Table S1: Stability of the serum samples after 6 months interval**

Patients ID	IRMA PTHrP Levels (pg/mL) 02/2015	IRMA PTHrP Levels (pg/mL) 08/2015
3244	15	12
3267	18	21
3494	90	90
3530	36	33
3609	14	15
3659	24	30

### Microfluidic Device

As previously reported by Otieno et al the microfluidic system featured two devices; detection chamber and capture chamber.<sup>2</sup> The detection chamber (Figure S1A) features a molded, soft PDMS 1.5 mm wide rectangular channel placed on top of the electrode array. The microfluidic channel was supported by two flat poly(methylmethacrylate) (PMMA) plates manufactured to fit on both sides of the PDMS slab and bolted together to seal the microfluidic channel 1.5 mm wide, 2.8 cm long, and 63  $\mu$ L in volume. The top PMMA plate contained female ports (4 mm diameter) for screwing in male plastic fittings to hold 0.2 mm i.d. PEEK tubing for inlet and outlet purposes. The top PMMA plate also contained 0.6 mm holes to hold Ag/AgCl and 0.2 mm holes for Pt wire electrodes. The capture chamber (Figure S1B), on the other hand, features a PDMS channel with an oval cylindrical channel housing a tiny magnetic stir bar. The PDMS channel is sandwiched between two PMMA plates to form a channel that is 100  $\mu$ L in volume. For the microfluidic system, a Harvard pump 11 elite model 70-4501 syringe pump was used. The pump was connected to the inlet through a Rheodyne model 9725i injector valve with sample loop of 100  $\mu$ L through 0.2 mm i.d. tubing (Figure 1, main paper).

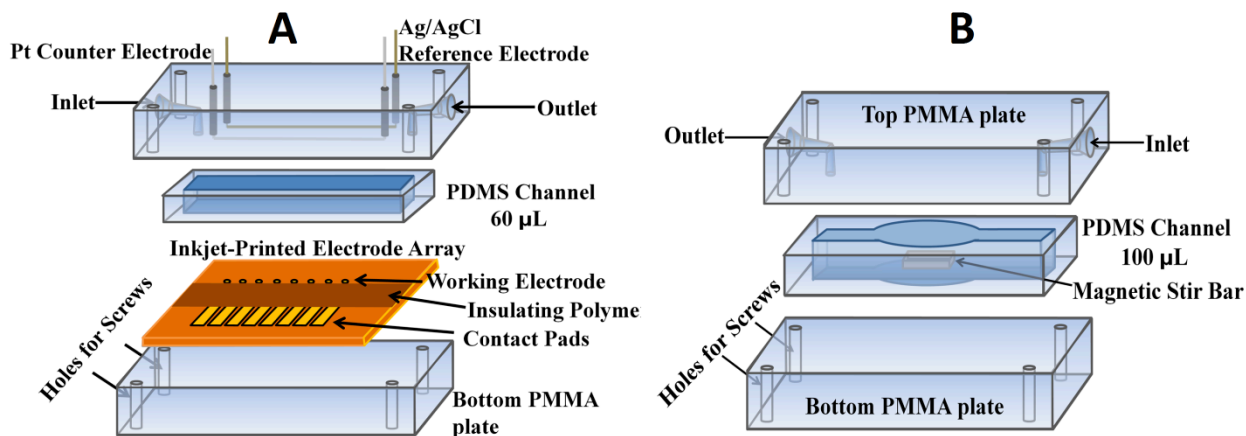


Figure S1: Components of the microfluidic device (A) detection chamber and (B) capture chamber made of micro-machined PMMA, PDMS microfluidic channel and inkjet-printed gold electrode array.

### Production of Gold Immunoarrays

Gold Array Fabrication followed previously established protocols by Jensen et al.<sup>3</sup> Gold nanoparticle ink was prepared at 100 mg/mL in toluene and filtered using a 0.2 mm cutoff PTFE filter. The ink was then injected into a Dimatix cartridge for use in the Dimatix Inkjet materials printer. Upon printing the gold, the arrays were sintered for 15 minutes at 200°C. The arrays lightened in color indicating the loss of the dodecane thiol layer and Au cores coalescing. Immediately after being sintered the arrays were returned to the Dimatix Inkjet materials printer to print the poly(amic acid) insulation layer. The poly(amic acid) ink was prepared, as previously reported, by diluting the 10% (m/m) poly(amic acid) solution in pure N-methyl-2-pyrrolidone (NMP) to 1% (m/m) and the adding the solution to a liquid crystal Dimatix printer cartridge immediately prior to use.

### Array Fabrication

Immunoarrays were fabricated from 4 nm dodecanethiol decorated gold nanoparticles (AuNPs) on Kapton sheet as previously described<sup>3</sup> using Dimatix inkjet materials printer. The inkjet-printed electrode arrays were annealed to drive off the thiol layer and then insulated with poly(amic acid), a Kapton precursor layer. The electrode arrays were then cleaned in 0.18 M sulfuric acid, by cycling potential between 1.5 and -0.2 V vs. saturated calomel electrode (SCE)

to remove gold oxide from the surface. The electrode arrays were coated with self assembled monolayer (SAM) of mercaptopropionic acid (MPA) to introduce carboxyl groups on the surface of the array. The surface carboxyl groups were activated by freshly prepared EDC and NHSS to attach monoclonal antibodies ( $Ab_1$ ) to array elements through amidization overnight. The arrays-modified with  $Ab_1$  were then washed with PBS-T20 to remove excess unbound  $Ab_1$  and incubated with 2% BSA for 1 hr to minimize non-specific binding (NSB). The  $Ab_1$ -modified arrays were then fitted into the detection chamber for amperometric measurement. A new array was employed for each measurement.

### Derivatization of Magnetic Beads

Magnetic bead bioconjugates [tosyl-activated magnetic beads (MBs)-Horseradish peroxidase (HRP)- Antibody ( $Ab_2$ )] were prepared using as previously described<sup>4</sup> with slight modification to reduce the bead conjugate preparation time from 42 to 24 hr. Briefly, tosylactivated magnetic beads (MB) (0.2 mg) were washed 3x with sodium borate buffer (pH 9.5), then reconstituted in 3 M ammonium sulfate + 0.1 M sodium borate buffer (volume 1:1). Horseradish peroxidase (HRP) (3 mg) and polyclonal antibody ( $Ab_2$ ) (0.8 mg) were then simultaneously added to the dispersion and incubated at 37 °C for 18 hrs. The magnetic bead bioconjugates (HRP-MB- $Ab_2$ ) were then washed with PBS-T20 and reconstituted in 0.5% BSA at 37 °C for 6 hrs to block NSB. The resulting beads were washed 3x with 0.1% BSA, reconstituted in 600  $\mu$ L of 0.1% BSA and stored at 4 °C. The number of  $Ab_2$  per MB was estimated to be  $(4-11) \times 10^4$  for different polyclonal antibodies for PTHrP using a protein assay kit (Bicinchoninic acid assay, BCA). Activity assays showed that the number of HRP per MB was  $(1.3-2.6) \times 10^5$  (Table S2).

**Table S2: Characterization of Magnetic Bead Conjugate**

Antibodies ( $Ab_2$ )	ABTS (#HRP per bead)	BCA (# $Ab_2$ per bead)
MA45	256,000 $\pm$ 20,000	40,000 $\pm$ 6,000
IgY 3103	165,000 $\pm$ 19,000	96,000 $\pm$ 7,000
IgY 3104	127,000 $\pm$ 5,000	114,000 $\pm$ 11,000

The Bicinchoninic acid (BCA) protein assay kit (Thermo Scientific, IL, USA) was used to access the number of Ab<sub>2</sub> molecules per MB<sub>tosyl</sub> estimated from the amount left in solution after MB<sub>tosyl</sub>-Ab<sub>2</sub> conjugation and compared to a standard curve of Ab<sub>2</sub> (Table S2).<sup>5,6</sup> The number of horseradish peroxidase labels per magnetic beads determined by measuring enzyme activity using 2,2'-Azino-bis(3-Ethylbenzthiazoline-6 Sulfonic Acid) (ABTS) as reactant (Table S2).<sup>7</sup>

### **Detection of PTHrP isoforms and their fragments encompassing the N-terminus and C-Terminus**

The semi-automated microfluidic system was constructed as previously reported<sup>2</sup> (Figure 1, main paper) and electrochemical measurements were all done at room temperature with a CHI 1040A eight-channel potentiostat at conditions optimized for high sensitivity and low S/N. The capture and detection chamber were first connected to the microfluidic system and subjected to a flow of PBS-T20 to block for NSB. 30  $\mu$ L of HRP-MB-Ab<sub>2</sub> conjugate was reconstituted in 130  $\mu$ L of 20 mM PBS buffer (pH 7.4), loaded into the 100  $\mu$ L sample loop and injected into the capture chamber at 100  $\mu$ L/min flow rate. 5  $\mu$ L of PTHrP standard reconstituted in 5x diluted calf serum was loaded into the sample loop and injected into the capture chamber. HRP-MB-Ab<sub>2</sub> conjugate were held in the capture chamber, through use of a neodymium magnet positioned above the top PMMA plate, as the peptide standard or serum/plasma sample was injected. For simultaneous detection of N-terminal (1-33 or 1-86), and C-terminal peptides (151-169, 140-173) or intact 1-173 isoform, 10  $\mu$ L of HRP-MB-Ab<sub>2</sub> conjugate for each peptide was reconstituted in 130  $\mu$ L of PBS buffer, loaded into the sample loop and injected into the capture chamber followed by injection of a mixture of the three standard peptides diluted in calf serum. Flow was then stopped, magnet removed and incubation was allowed for 30 mins with stirring for the peptide to be captured by HRP-MB-Ab<sub>2</sub> conjugate.

The resulting peptide-Ab<sub>2</sub>-MB-HRP conjugates were washed by flushing the capture chamber with PBS-T20 while holding the magnet bar on top of the PMMA plate and then re-dispersed in PBS-T20. The direction of flow was changed and the peptide-Ab<sub>2</sub>-MB-HRP conjugates were transported into the detection chamber housing the Ab<sub>1</sub>-modified 8-electrode array. After peptide-Ab<sub>2</sub>-MB-HRP conjugates filled the detection chamber, flow was stopped



and incubation was allowed for 15 mins for Ab<sub>1</sub> on the array to capture the bead conjugate. Unbound bead conjugate was then washed off by resuming buffer flow.

To perform amperometric measurements, the arrays were further subjected to a flow of buffer containing 1 mM hydroquinone in PBS for 4 mins. The 8 electrodes of the array were then connected to the working electrode leads of a CHI 1040 multi-potentiostat, and the Pt and Ag/AgCl wires were connected to the counter and reference leads, respectively. Amperometric detection was performed at -0.3 V vs Ag/AgCl by injecting a mixture of 1 mM hydroquinone and 0.1 mM hydrogen peroxide into the detection chamber via the sample loop at 100  $\mu$ L/min. Hydrogen peroxide activates HRP on the peptide-Ab<sub>2</sub>-MB-HRP conjugates to ferrioxo-HRP, which, in turn oxidizes hydroquinone to benzoquinone. Signal is generated as benzoquinone is reduced through a 2-electron transfer at the electrode surface.

### **Optimization of Polyclonal and Monoclonal Antibodies**

To establish optimal conditions for the assays as well as to improve on both the signal to noise ratio and sensitivity, polyclonal antibodies on the surface of the arrays and monoclonal antibodies on the conjugate magnetic beads were optimized. N-terminal fragments (1-33 & 1-86) were paired with antibodies PA158 and MA45, while the C-terminal fragments (151-169 & 140-173) were paired with antibodies (PA6 & PA104) and (IgY3103 & IgY3104). We began with optimizing the antibody concentrations on the magnetic beads keeping a consistent Ab<sub>1</sub> antibody concentration of 100  $\mu$ g/mL, and employing standard concentration of 0, 2.5, and 5 pg/mL for standard peptide fragments (of 151-169, 140-173, and 1-33). The optimal secondary antibody concentration was determined from the greatest signal difference between the control and sample concentration for IgY3103 50  $\mu$ g/mL, for IgY3104 50  $\mu$ g/mL, and for M45 20  $\mu$ g/mL (Figure S2 A,B,C). Once the secondary antibody concentration was confirmed for the conjugate magnetic beads the optimal concentration of primary antibody on the surface of the arrays was established using a consistent optimized secondary antibody concentration (IgY3103 50  $\mu$ g/mL, IgY3104 50  $\mu$ g/mL, and M45 20  $\mu$ g/mL) again employing standard concentrations of 0, 2.5, and 5 pg/mL for standard peptide fragments (of 151-169, 140-173, and 1-33). The greatest signal difference between control and sample concentration indicated the optimal primary antibody concentration to be 100  $\mu$ g/mL for all polyclonal antibodies (Figure S2 D,E,F).

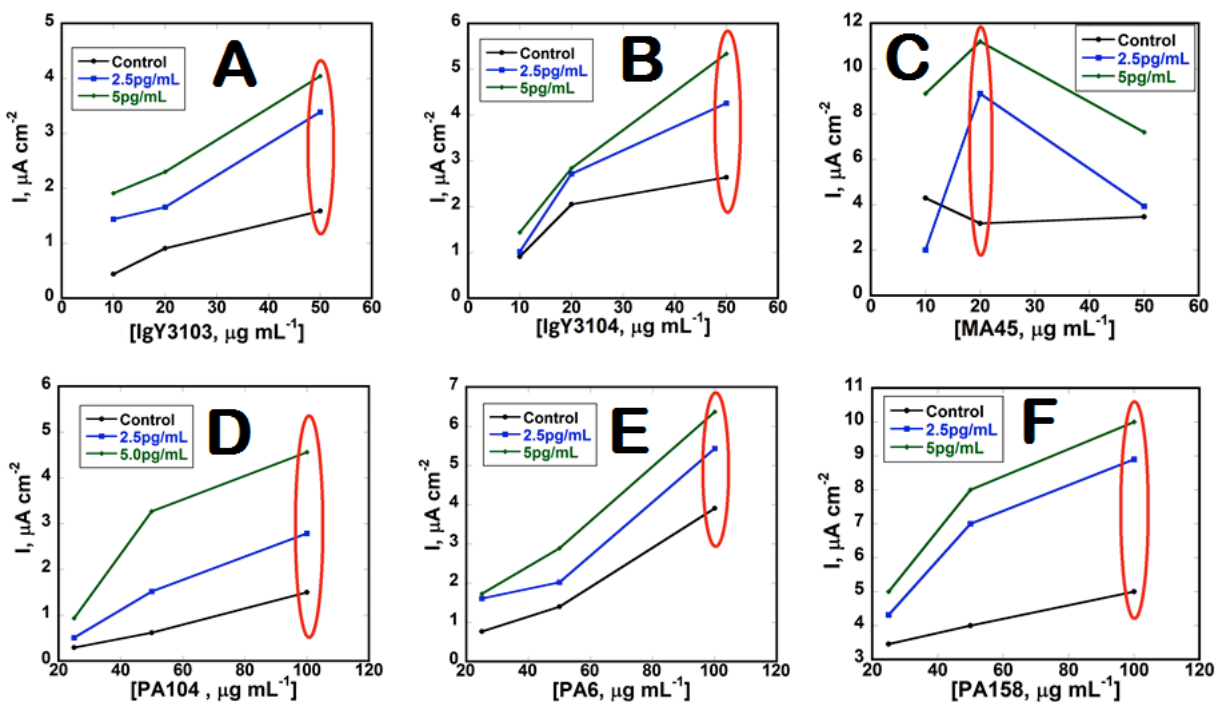


Figure S2: Optimization of monoclonal antibody ( $Ab_2$ ) and polyclonal antibody ( $Ab_1$ ) concentration using a control and standard concentrations of 2.5, 5 pg/mL for (A) MA3103, (B) MA3104, (C) MA45, (D) PA104, (E) PA6, and (F) PA158. Optimal concentrations for both  $Ab_1$  and  $Ab_2$  are circled.

### Evaluation of the Assay Performance

Generally robust analytical requirements (linearity, inter-assay precision, intra-assay precision, absence of a carry-over effect) were fulfilled and reproducibility was good. Inter-assay precision was determined by running the same concentration of two standards on different batches of arrays. On the other hand, intra-assay variation was determined by measuring the variation within the 8-electrode array on same batch. In each case, samples were run in triplicate for each run, with two separate runs each day for 5 days. The inter-assay relative precision was <7% and intra-assay precision was <5% (Table S3). The Linear dynamic range of the assay was assessed by running peptide standards in 5x diluted calf serum as well as by running human serum samples at different dilutions. The peptide standards gave linear responses from 0.003 to 16 pg/mL (0.15 fmol/L to 7 pmol/L). Each sample was run in triplicate and averaged. The assay

limit of detection was established from the signal of the control (5x diluted calf serum) plus 3x the standard deviation of that signal. Correlation plots were used to evaluate the comparison with the referee IRMA method. The microfluidic system was subjected to PBS-T20 wash for 4 mins before and after each standard run to minimize NSB and carry-over effects (Figure S3). Analytical recovery of the assay was also evaluated by spiking the diluted calf serum with peptide standards. Analytical recovery above 80% was obtained.

**Table S3: Evaluation of Assay Performance**

<b>Assay Parameters</b>	<b>Results</b>
<b>Limit of Detection (3x stdev + Control)</b>	<b>3 fg/mL</b>
<b>Dynamic Range (Linearity in 5x diluted calf serum)</b>	<b>3 fg/mL to 16 pg/mL</b>
<b>Inter-assay variation</b>	<b>7%</b>
<b>Intra-assay variation</b>	<b>5%</b>
<b>Analytical Recovery</b>	<b>&gt;80%</b>

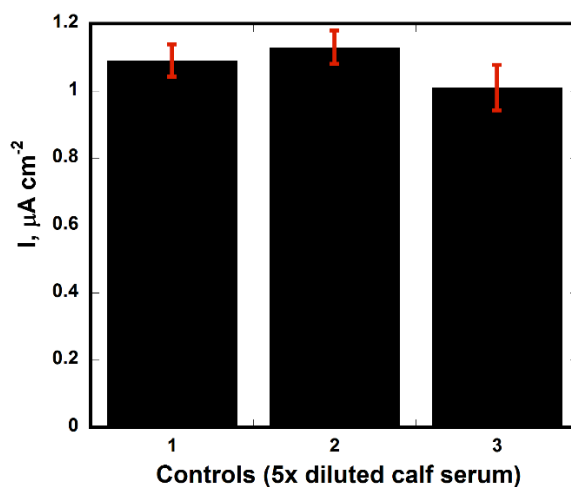


Figure S3: Controls (5x diluted calf serum) run at the beginning of the assay (1), after running 3 pg/mL peptide standard (2) and at the end of the day after running high concentration (16 pg/mL) of peptide standard (3). Illustrating minimal/no carry-over effect between runs.

## Amperometric peaks for Individual Peptide fragments

Additional amperometric responses for individual standard peptide fragments (1-33, 151-169, and 140-173) developed by injecting a mixture of 1 mM HQ and 0.1 mM hydrogen peroxide at -0.3V are shown in Figure S4. Control experiments feature the full assay protocol without peptide analyte. Control signals are a consequence of a combination of direct reduction of hydrogen peroxide and NSB of the labeled bioconjugate beads on the sensors. The corresponding calibration curves are reported in Figure 2 of the main paper. A full report of detection limits and sensitivities of these calibration curves is shown in Table S4. The dynamic range of the assay can be extended by tailoring assay parameters such as incubation time and number of enzyme labels on the magnetic beads.

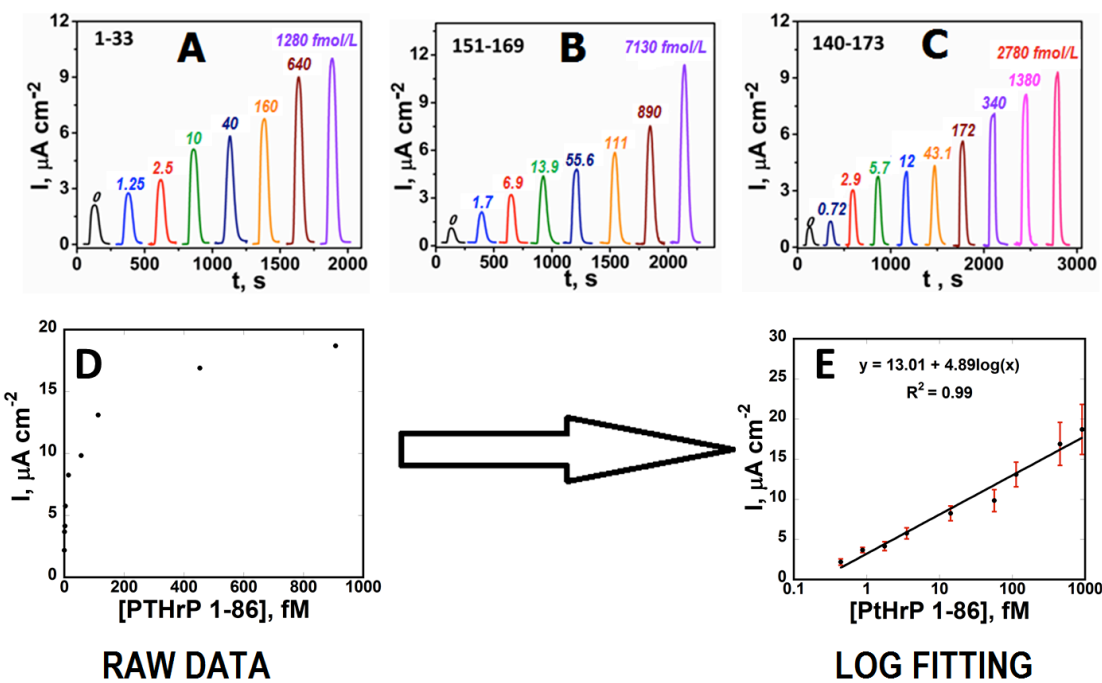


Figure S4: Amperometric response for individual peptide fragment A) 1-33, B) 151-169 and C) 140-173 at -0.2 V by injecting a mixture of HQ and  $\text{H}_2\text{O}_2$ . Raw data of PTHrP 1-86 (D) and log fitted data (E) is also shown.

## Specificity Assay

Based on the sensitivities observed during single peptide detection, the larger peptide fragments (1-86 & 1-173) were selected for multiplexed detection (Table S4). Employing the 8-electrode array, a sandwich assay was build up on the first three electrodes for detection of 1-173

using PA104 and IgY3103, the next three electrodes for detection of 1-86 using PA158 and MA45 and the last two electrodes for detection of 1-173 using PA6 and IgY3104 (Figure S5A). Magnetic bead conjugate (10  $\mu$ L each) with MA45, IgY3103 and IgY3104 were combined, dispersed in PBS and injected into the capture chamber via the sample loop. A mixture of standards for 1-86 and 1-173 (volume ratio 1:2) was then introduced into the capture chamber with the aid of the magnet bar positioned above the capture chamber. All steps, from washing the resulting peptide-bead conjugate to amperometric detection, were performed as illustrated above for single peptide detection. Prior to obtaining calibration plots, binding studies were done to determine the specificity of the antibodies towards the peptide fragments (Figure S5B). Minimal cross-reactivity was observed between the antibodies for 1-173 and 1-86 peptide analytes.

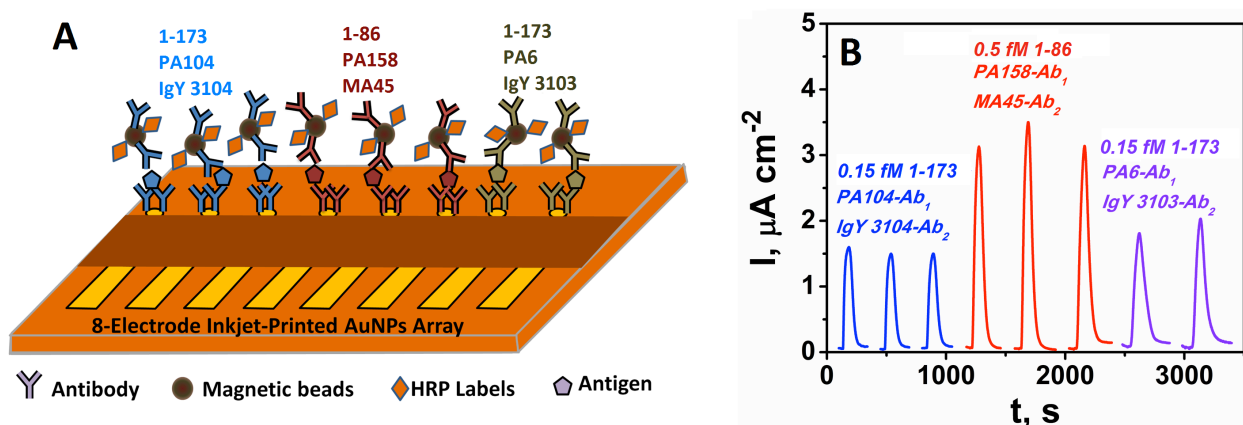


Figure S5: A) Multiplexing strategy for the peptide fragments on a single 8-electrode inkjet-printed AuNPs array. B) Representative amperometric response for detection of a mixture of 1-173 and 1-86 on a single 8-electrode array.

## ROC Analysis

Analysis of the patient PTHrP data was also done using Receiver Operating Characteristic (ROC) plots. ROC is commonly used in clinical tests to determine the accuracy of the test and obtain cut-off values in diagnostic tests. In ROC curves, sensitivity (true positive rate) is plotted against 100-specificity (false positive rate) for different cut-off points. Each point on the ROC curve represents a sensitivity/specificity pair corresponding to a particular decision threshold. A test with perfect discrimination has a ROC curve that passes through the upper left corner (100% sensitivity, 100% specificity).<sup>8</sup> Therefore, the closer the ROC curve is to the upper

left corner, the higher the overall accuracy of the test. The area under a ROC curve (AUC) quantifies the overall ability of the test to discriminate between those individuals with the disease and those without the disease. A truly perfect test with zero false positives and zero false negatives has an AUC of 1.00.

Using the PTHrP data from the 57 samples, ROC plot had an AUC of 0.96 and 0.94 for PTHrP levels detected using 1-86 fragment and intact 1-173, respectively. 1-86 fragments gave 80% sensitivity and 100% specificity while intact 1-173 gave 82.86% sensitivity and 95.45% specificity. T-tests showed a significant difference between the PTHrP levels in cancer and control samples (Figure 6) ( $P < 0.001$ ). The cut-off value for PTHrP level in cancer vs non-cancer patients was found to be  $>10.91$  pg/mL (1.1 pmol/L) using 1-86 fragment which in agreement with the IRMA results.

**Table S4: Detection Limit and Sensitivity**

Peptide Fragments	Antibody on the Sensor	Antibody on the Beads	Single Detection (DL fg/mL)	Sensitivity ( $\mu\text{A}/\text{cm}^2$ )/(C)	Fragment size (no. of aa)
1-33	PA158	MA45	5 (1.25 fM)	2.22	33
151-169	PA6	IgY3103	4 (1.7 fM)	2.12	19
140-173	PA104	IgY3104	3 (0.72 fM)	1.98	33
1-86	PA158	IgY3103	4 (0.44 fM)	4.89	86
1-173	PA104	IgY3104	3 (0.15 fM)	3.55	173

**Table S5: Serum Samples Data**

	Number of Samples (n)	Mean PTHrP (pg/mL)	Stdev
Healthy Individuals	22	6.69 (0.68 pM)	2.07
Cancer Patients	35	23.99 (2.42 pM)	22.77

**Table S6: Correlation plot table:** Illustrating the slope and intercept obtained from serum samples in Figure 4 (main paper).

PTHrP	Slope	Intercept	R <sup>2</sup>
1-86	$0.90 \pm 0.02$	$0.13 \pm 0.05$	0.99
1-173	$0.40 \pm 0.01$	$0.02 \pm 0.019$	0.99

## Electrode Surface Area Calculation

Prior to each immunoassay, each of the bare gold arrays were cleaned in 0.18M sulfuric acid, by applying 20 sweep segments between 1.5 V and -0.2 V at 100 mV s<sup>-1</sup>. Figure 7 shows similar peaks to those found from bulk gold with formation of gold oxide at +1.2 V and reduction back to bulk gold occurring at 0.9 V.<sup>9</sup> From these CVs, the active surface area was calculated following Trasatti et al.<sup>10</sup>

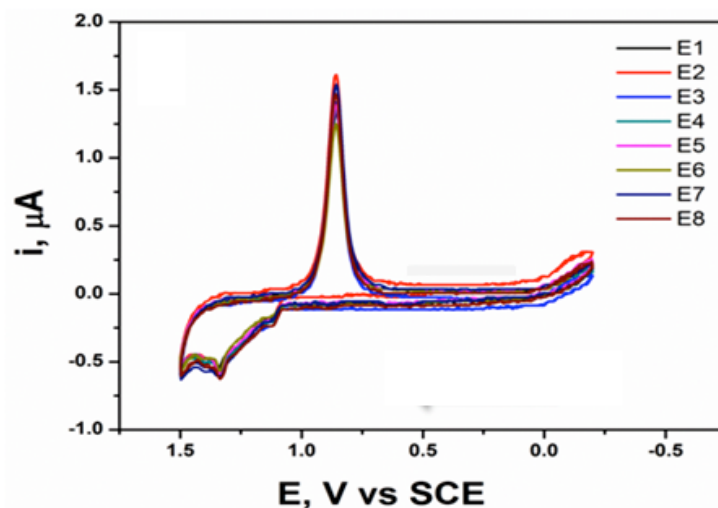


Figure S6: Cyclic voltammogram obtained by cycling the 8-electrode gold arrays in 0.18 M H<sub>2</sub>SO<sub>4</sub>. Electrode surface area is calculated by integrating the area under the curve.

## REFERENCES

1. Kremer, R.; Huang, D. C. PTHRP, its isoforms and antagonists thereto in the diagnosis and treatment of disease. US patent# 7,897,139B2 Issued March 1, **2011**.
2. Otieno, B. A.; Krause, C. E.; Latus, A.; Chikkaveeraiah, B. V.; Faria, R. C.; Rusling, J. F. *Biosens. Bioelectron.* **2014**, *53*, 268-74.
3. Jensen, G. C.; Krause, C. E.; Sotzing, G. A.; Rusling, J. F. *Phys. Chem. Chem. Phys.* **2011**, *13*, 4888-94.
4. Krause, C. E.; Otieno, B. A.; Latus, A.; Faria, R. C.; Patel, V.; Gutkind, J. S.; Rusling, J. F. *ChemistryOpen* **2013**, *2*, 141-5.

- 
5. Smith, P. K.; Krohn, R. I.; Hermanson, G. T.; Mallia, A. K.; Gartner, F. H.; Provenzano, M. D.; Fujimoto, E. K.; Goeke, N. M.; Olson, B. J.; Klenk, D. C. *Anal. Biochem.* **1985**, *150*, 76-85.
  6. Wiechelman, K. J.; Braun, R. D.; Fitzpatrick, J. D. *Anal. Biochem.* **1988**, *175*, 231-7.
  7. Chikkaveeraiah, B. V.; Mani, V.; Patel, V.; Gutkind, J. S.; Rusling, J. F. *Biosens. Bioelectron.* **2011**, *26*, 4477-83.
  8. Zweig, M. H.; Campbell, G. *Clin. Chem.* **1993**, *39*, 561-77.
  9. Cadle, S. H.; Bruckenstein, S. *Anal. Chem.* **1974**, *46*, 16-20.
  10. Trasatti, S.; Petrii, O. A. *Pure Appl. Chem.* **1991**, *63*, 711-34.